Int. J. Multiphase Flow Vol. 15, No. 1, pp. 51–64, 1989
Printed in Great Britain.
0301-9322/89 $3.00 + 0.00

PRESSURE LOSSES CAUSED BY AREA CHANGES IN A SINGLE-CHANNEL FLOW UNDER TWO-PHASE FLOW CONDITIONS

A. TAPUCU,[1] A. TEYSSEDOU,[1] N. TROCHE[1] and M. MERILO[2]
[1]Ecole Polytechnique, 2900 Eduard Montpetit, Montréal, Québec H3T 1J4, Canada
[2]Electric Power Research Institute, California, U.S.A.

(*Received* 27 *July* 1987; *in revised form* 8 *September* 1988)

Abstract—Experimental data obtained on plate and smooth blockages under two-phase flow conditions in a square vertical channel have been presented and analysed using the Janssen–Kervinen and momentum–energy models. The vena contracta coefficients obtained for plate blockages using these models agree well up to about 30% void fraction. It is observed that the contraction coefficients for two-phase flow differ somewhat from those for single-phase flows. The irreversible pressure loss coefficients for plate and smooth blockages depend on blockage severity and void fraction.

Key Words: two-phase, blockages, pressure drop, irreversible pressure drop

1. INTRODUCTION

The optimal safe operation of many processes requires the evaluation of the two-phase pressure drop associated with enlargements, contractions, orifices, inserts etc. The problem is particularly important in natural circulation units and in safety analysis of nuclear reactors. Despite the sizable amount of data collected, an accurate prediction of this pressure drop has not yet been achieved. The aim of this paper is to review the calculation of pressure drops caused by singularities in a channel, and to present irreversible pressure drop data for plate and smooth blockages along with the axial distribution of pressures and void fractions in a square vertical channel.

2. LITERATURE SURVEY ON THE ESTIMATION OF IRREVERSIBLE PRESSURE LOSSES

Sudden enlargement

Consider the enlargement illustrated in figure 1. Fluid emerging from the smaller pipe is unable to follow the abrupt deviation of the boundary. Consequently, pockets of eddies form in the corners and result in the dissipation of mechanical energy as heat. The determination of the irreversible component of the total pressure drop requires the use of the momentum and energy conservation equations. The total pressure drop (reversible and irreversible) between planes 1 and 2 in figure 1 is obtained by applying the momentum equation to the volume limited by these planes and the walls of the pipe. It is also assumed that the wall friction is negligible, and the pressures and velocities of each phase in planes 1 and 2 are uniform. In turn, the viscous term appearing in the energy equation is identified as the irreversible component of the total pressure drop. This general approach has been used by Kays (1950), Hewitt & Hall Taylor (1970), Collier (1972) and Delhaye (1981), among others, to determine the irreversible pressure loss under single-phase and two-phase flow conditions. The local conservation equations for a steady-state two-phase flow are given below:

(*a*) *mass*,

$$\frac{\partial}{\partial z}(AG) = 0; \qquad [1]$$

(*b*) *momentum*,

$$\frac{\partial}{\partial z}(AG^2 v') + A\frac{\partial p}{\partial z} = -p_w \tau_w - A\bar{\rho} g, \qquad [2]$$

where v' is the momentum specific volume and is defined as

$$v' = \frac{x^2}{\epsilon\rho_G} + \frac{(1-x)^2}{(1-\epsilon)\rho_L};$$

and

(*c*) *energy*,

$$\frac{\partial}{\partial z}\left(A\frac{G^3 v''^2}{2}\right) + \frac{\partial}{\partial z}\left(\frac{AG}{\rho_H}p\right) - \frac{\partial}{\partial z}(A\phi') = 0, \qquad [3]$$

where

$$v''^2 = \frac{x^3}{\epsilon^2\rho_G^2} + \frac{(1-x)^3}{(1-\epsilon)^2\rho_L^2},$$

$$\frac{1}{\rho_H} = \frac{x}{\rho_G} + \frac{(1-x)}{\rho_L}$$

and ϕ' is the viscous dissipation.

Integrating [2] and [3] over the control volume shown in figure 1 and combining the resulting equations the irreversible pressure loss can be written as

$$\Delta p_{I,\exp} = G_1^2(1-\sigma)\left\{\sigma\left[\frac{x^2}{\epsilon\rho_G} + \frac{(1-x)^2}{(1-\epsilon)\rho_L}\right] - \frac{\rho_H}{2}(1+\sigma)\left[\frac{x^3}{\epsilon^2\rho_G^2} + \frac{(1-x)^3}{(1-\epsilon)^2\rho_L^2}\right]\right\}. \qquad [4]$$

Janssen & Kervinen (1964) assumed that the total pressure change, $(p_2 - p_1)_T$, is given by

$$(p_2 - p_1)_T = (p_2 - p_1)_R + \Delta p_I - \Delta p_F, \qquad [5]$$

where $(p_2 - p_1)_R$ is the reversible pressure change and Δp_I and Δp_F are irreversible pressure drops due to expansion and wall friction, respectively. The reversible pressure change is estimated by

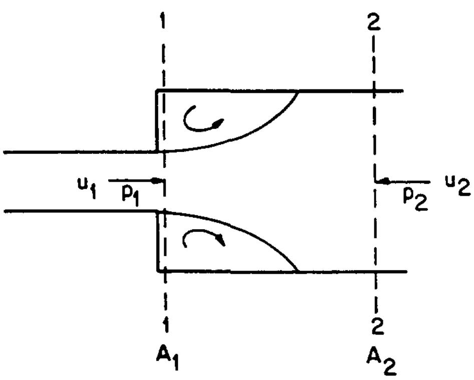

Figure 1. Sudden enlargement.

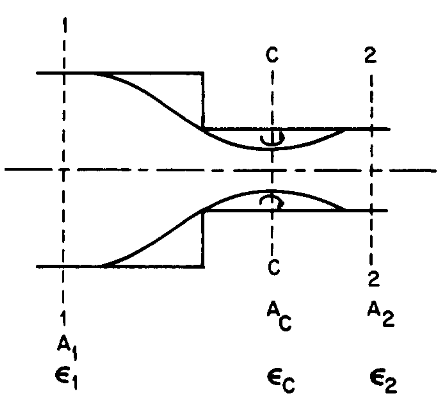

Figure 2. Sudden contraction.

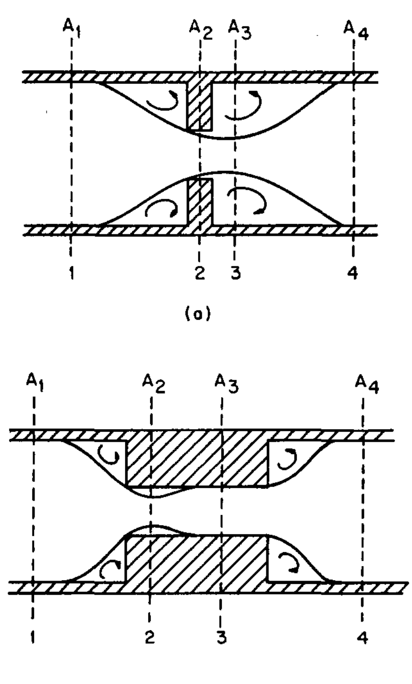

Figure 3. Sharp inserts: (a) short insert; (b) long insert.

integrating [2] in a duct of varying flow section with the assumption of negligible wall friction, while the term $(p_2 - p_1)_T + \Delta p_F$ is estimated by integrating the same equation over the control volume seen in figure 1. Assuming a constant void fraction along the duct, the irreversible pressure loss has the following form:

$$\Delta p_{I,\,exp} = -\frac{1}{2}\frac{G_1^2}{\rho'}(1-\sigma)^2 \qquad [6]$$

where $\rho' = 1/v'$ is the momentum density. Even though the use of the momentum density is consistent with the actual theoretical model, Morris (1984) suggested a correction to take into account the liquid entrained by the gas in the evaluation of momentum flux. When the effective specific volume v_e defined by Morris is compared with the present momentum specific volume ($v' = 1/\rho'$) the observed differences are of the same order of magnitude as the experimental errors ($+5\%$).

Sudden contraction

Immediately downstream of the area change a vena contracta is formed (figure 2). After the vena contracta, the flow widens to fill the pipe. Eddies formed between the vena contracta and the wall of the pipe cause practically all the dissipation of energy. Therefore, it is usually assumed (Kays 1950; Hewitt & Hall Taylor 1970; Collier 1972; Delhaye 1981) that the contraction of the fluid to the vena contracta (plane C) is reversible and the irreversible pressure drop takes place only in the region of the flow expansion from the vena contracta to the flow section of the smaller tube. Using the above approximation and [4], the irreversible pressure drop for an incompressible flow with constant void fraction along the duct is given by

$$\Delta p_{I,\,con} = G_2^2\frac{1-C}{C^2}\left\{C\left[\frac{x^2}{\epsilon\rho_G}+\frac{(1-x)^2}{(1-\epsilon)\rho_L}\right]-\frac{(1+C)\left[\frac{x^3}{\epsilon^2\rho_G^2}+\frac{(1-x)^3}{(1-\epsilon)^2\rho_L^2}\right]}{2\left[\frac{x}{\rho_G}+\frac{(1-x)}{\rho_L}\right]}\right\} \qquad [7]$$

where $C\ (=A_C/A_2)$ is the contraction coefficient and $\sigma = A_1/A_2$.

Similarly, applying [6] to the expansion from the vena contracta to the flow section of the smaller tube, the following equation is obtained for the irreversible pressure drop:

$$\Delta p_{I,\,con} = \frac{1}{2}\frac{G_2^2}{\rho'}\left(\frac{1}{C}-1\right)^2. \qquad [8]$$

Sharp insert

Sharp inserts are defined as a sudden contraction in a channel followed by a sudden expansion. Depending on the distance between the contraction and the expansion, the inserts are classified as long or short [figure 3(a,b)]. With short inserts, the vena contracta forms outside of the restriction while for long inserts, it forms within the length of the restriction.

Contraction and expansion losses cannot be separated in the case of short inserts. However, Janssen & Kervinen (1964), assuming that the contraction losses are small compared to the expansion losses [from the vena contracta, A_3, to the channel flow section, A_4; figure 3(a)] and that the pressure p_3 acts uniformly on the plane 3 containing the vena contracta, established the following relationship for the irreversible pressure loss:

$$\Delta p_{SI} = -\frac{G_1^2}{2\rho_L}\left(\frac{1}{\sigma^2C^2}\right)\left\{\frac{\rho_L}{\rho_G}x^2\bar{\epsilon}\left[\left(\frac{1}{\epsilon_3}\right)^2-\left(\frac{\sigma C}{\epsilon_4}\right)^2\right]+(1-x)^2(1-\bar{\epsilon})\left[\left(\frac{1}{1-\epsilon_3}\right)^2-\left(\frac{\sigma C}{1-\epsilon_4}\right)^2\right]\right.$$
$$\left.-2\sigma C\left[\frac{\rho_L}{\rho_G}x^2\left(\frac{1}{\epsilon_3}-\frac{\sigma C}{\epsilon_4}\right)+(1-x)^2\left(\frac{1}{1-\epsilon_3}-\frac{\sigma C}{1-\epsilon_4}\right)\right]\right\}, \qquad [9]$$

where

$$\bar{\epsilon} = \frac{1}{2}(\epsilon_3 + \epsilon_4),$$

$$\sigma = \frac{A_2}{A_1} = \frac{A_2}{A_4}$$

and

$$C = \frac{A_3}{A_2}.$$

The assumption of a constant void fraction along the tube leads to

$$\Delta p_{SI} = -\frac{1}{2}\frac{G_1^2}{\rho'}\left(\frac{1}{\sigma C} - 1\right)^2. \qquad [10]$$

In turn, using the same assumption as Janssen & Kervinen (1964) and applying the momentum–energy approach as used by Hewitt & Hall Taylor (1970) for a sudden expansion, the following relationship results:

$$\Delta p_{SI} = G_1^2\left[\frac{1}{\sigma C}\left(\frac{1}{\rho_3'} - \frac{1}{\rho_4'}\right)\right] - \frac{G_1^2 \rho_H}{2}\left[\frac{1}{(\sigma C)^2}\left(\frac{1}{\rho_3''^2} - \frac{1}{\rho_4''^2}\right)\right], \qquad [11]$$

where

$$\sigma = \frac{A_2}{A_1}$$

and

$$C = \frac{A_3}{A_2}.$$

The homogeneous two-phase density ρ_H is calculated at the mid-plane conditions of the blockage.

The assumption of a constant void fraction along the channel yields

$$\Delta p_{SI} = \frac{G_1^2}{2}\left\{\frac{2}{\rho'}\left(\frac{1}{\sigma C} - 1\right) - \frac{\rho_H}{\rho''^2}\left[\frac{1}{(\sigma C)^2} - 1\right]\right\}. \qquad [12]$$

With long inserts, the flow in the contracted section of the channel becomes fully developed [figure 3(b)]. Consequently, the contraction and expansion losses can be separated and the irreversible pressure loss of a long insert may be predicted by a simple summation of pressure losses through the contraction and expansion (Janssen & Kervinen 1964).

Very limited data exists in the open literature on the irreversible pressure losses caused by inserts. Janssen & Kervinen (1964) conducted experiments to determine the pressure losses caused by short and long inserts in flow channels for steam–water mixtures for pressures between 4.14 and 9.65 MPa, flow rates from 340 to 2700 kg/m^{2}s and qualities from 0 to 90%. A study was also made to determine the void fractions and the flow pattern in the vicinity of the insert using high-speed movies. The authors observed a strong mixing as the flow contracts and the formation of a vena contacta just past the contraction inlet of a long insert or just downstream of a short one. The vena contracta area is found to be smaller for long contraction–expansion inserts than for short ones. The momentum equations developed for short, [9], and long inserts predicted the measured irreversible pressure losses with reasonable accuracy with a slip ratio >1 everywhere except for the vena contracta of long inserts where its value is equal to 1. Weisman *et al.* (1978) determined two-phase flow pressure losses across abrupt area changes (contraction, expansion and a combination of the two) and restrictions (short and long inserts). Freon-113 was used as the working fluid. The void fractions upstream and downstream of the perturbed area were measured by impedance voidmeters. The authors, using their own data and those of other investigators, showed that a one-dimensional momentum balance can be used to predict pressure losses across abrupt area changes, provided that the void fractions are estimated appropriately.

The effect of flow blockage geometry on the pressure drop, the void distribution and the flow pattern transition in horizontal two-phase flow has been studied by Salcudean *et al.* (1983a–c). The authors observed that the two-phase multiplier depends on the blockage shape and its location in the flow section. For a given blockage fraction, the largest values of the two-phase multiplier are produced by peripheral blockages and are due to the interception of the liquid phase by these blockages. The central blockages, since they intercept the gaseous phase, yielded lower values for the two-phase multiplier.

Orifices

Orifices are used by the process industry to measure and control the flow and to determine the dryness fraction. Consequently, a good deal of data exists on the pressure drop characteristics of orifices. Data under air–water flow conditions have been collected by Simpson *et al.* (1979, 1983), Fairhurst (1983) and Chen *et al.* (1986). Data for steam–water flows have been given by Hoopes (1957), Monroe (1958), Thom (1963), Bizon (1965) and Chisholm & Watson (1965), among others. Different approaches have also been proposed to estimate two-phase pressure drops caused by orifices (Chisholm 1967a,b, 1983; Fairhurst 1983; Simpson *et al.* 1983; Chen *et al.* 1986).

Smooth insert

An asymmetrical smooth insert is illustrated in figures 4(a,b). In the expansion region (between planes 2 and 4), the flow can separate from the surface of the insert [figure 4(a)]. It could also be argued that the separation point would move upstream with increasing insert severity. If the flow separation occurs in the upstream region of the mid-plane, the formation of a vena contracta downstream of this plane should be possible [figure 4(b)]. As a first approximation, it can be assumed that the irreversible pressure drop occurs during the expansion of the flow between planes 2 (mid-plane) and 4. Therefore, [10] or [11] may be employed to estimate this pressure drop.

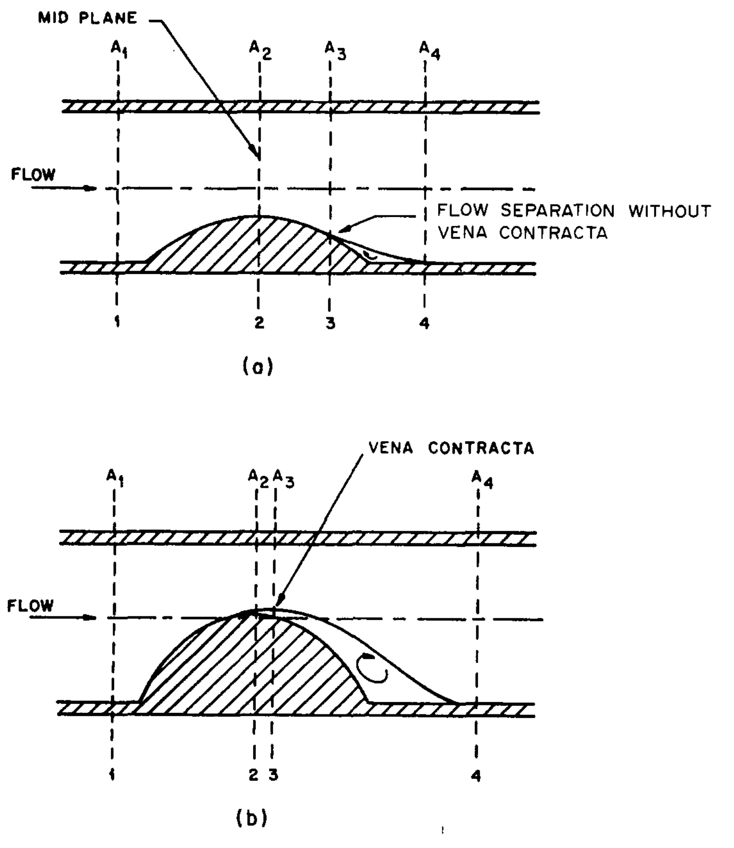

Figure 4. Smooth insert: (a) without formation of the vena contracta; (b) with formation of the vena contracta.

3. EXPERIMENTAL APPARATUS

The test section on which the blockage experiments have been conducted is made up of a 12.65 mm^2 channel machined from an acrylic block. Two blockage configurations were considered: plate and smooth. The shape of the latter blockage was a cosine. The plate blockage could be moved continuously in the radial direction to achieve any blockage fraction. Table 1 lists the geometric parameters of the blockages.

Table 1

Plate Blockage			
Area reduction (%)	21.0	41.5	61.3
Thickness, l (mm)	3.2	3.2	3.2
Height, h (mm)	2.7	5.3	7.5
Smooth Blockage			
Area reduction (%)	20.1	41.4	59.5
Length, L (mm)	51.0	51.0	50.0
Height, h (mm)	2.5	5.2	7.6

The main parameters measured are: inlet liquid and gas flow rates, axial pressures and average axial void fractions (by conductivity method) upstream and downstream of the blockage. The region over which the pressures are measured extends to 514 and 857 mm upstream and downstream of the mid-plane of the blockage. For void fraction this region extends to 323 mm upstream and 876 mm downstream of the blockage. Details on the experimental methods and the conditions under which the experiments have been conducted are given in Tapucu *et al.* (1988).

4. EXPERIMENTAL RESULTS

As a typical example, figures 5a and 5b give the pressure and void fractions measured upstream and downstream of a 40% plate blockage. Far from the blockage, the pressure varies linearly. A sudden pressure drop is observed in the blocked region. The different components of this pressure drop can be written as

$$\Delta p_{\mathrm{b}} = \Delta p_{\mathrm{form}} + \Delta p_{\mathrm{friction}} + \Delta p_{\mathrm{gravity}}; \qquad [13]$$

Δp_{form} is related to the dissipation of mechanical energy as heat in the recirculation zone behind the blockage and is equivalent to Δp_{SI} appearing in [9] and [11], $\Delta p_{\mathrm{friction}}$ is given by

$$\Delta p_{\mathrm{friction}} = \int \phi_L^2 \left(\frac{\mathrm{d}p}{\mathrm{d}z}\right)_{\mathrm{fo}} \mathrm{d}z .$$

The acceleration pressure loss caused by the expansion of the gas with the sudden decrease of the pressure in the blocked region is incorporated in the form pressure drop. Since the thickness of the plate blockage is small, the friction and gravity terms can be neglected and Δp_{b} becomes approximately equal to Δp_{form}. However, this does not hold true for a smooth blockage where the length is 50 mm. Therefore, the friction and gravity pressure loss terms should be evaluated adequately and subtracted from Δp_{b} to determine Δp_{form}. For plate blockages, the irreversible form pressure drop, $\Delta p_{\mathrm{form}} \approx \Delta p_{\mathrm{b}}$, is obtained by extrapolating the linear pressure variations upstream and downstream of the blockage to the mid-plane of the blockage (figure 5a). For smooth blockage, this pressure drop is obtained by extrapolating these linear pressure variations to the lower and upper planes which limit the blockage. Data on pressure drops caused by different blockages are given in Tapucu *et al.* (1988).

As can be seen from figure 5b, the void fractions in the far upstream and downstream regions of the blockage are almost uniform. Due to the pressure drop along the channel, the value of the void fraction far downstream of the blockage is somewhat higher than that in the far upstream region. In general, close to the blockage in the upstream region the void fraction shows a slight decrease. However, immediately downstream of the blockage, a high void fraction region is observed. This region is probably a consequence of the rather large bubbles trapped in the

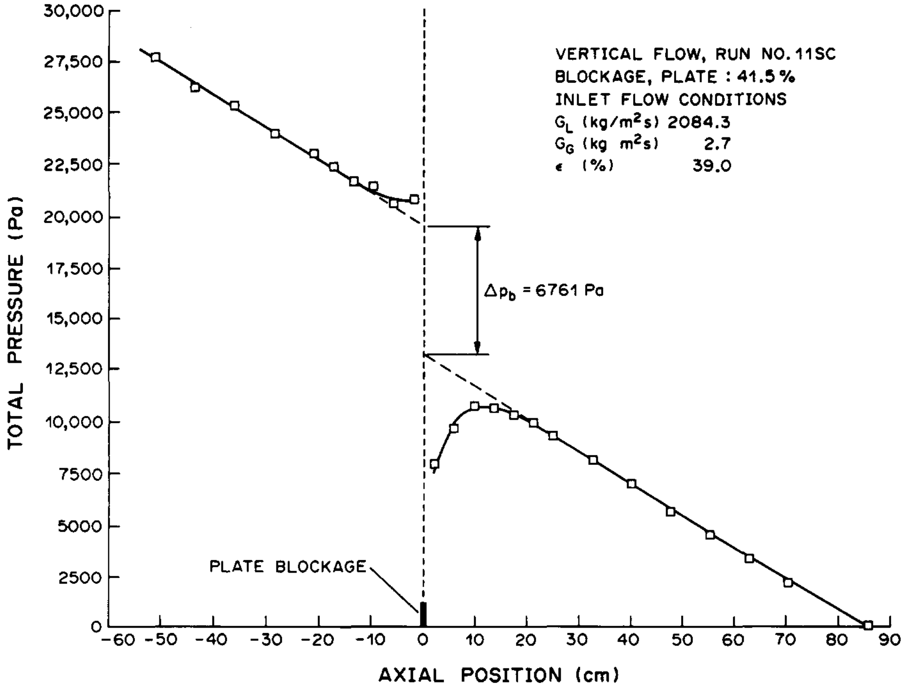

Figure 5a. Pressures upstream and downstream of a plate blockage.

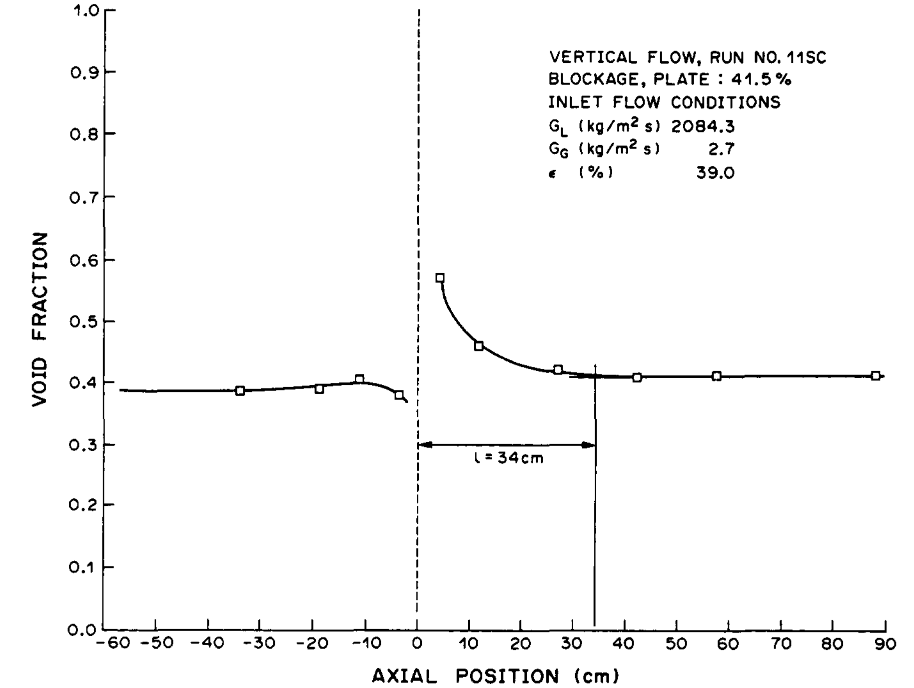

Figure 5b. Void fractions upstream and downstream of a plate blockage.

recirculation zone which develops behind the blockage. The length of the high void region, l, is estimated by examining the axial void profiles, similar to that given in figure 5b, and determining the point where the void fraction behind the blockage reaches its asymptotic value. Figure 6 gives the variation of the length of the high void region as a function of the blockage fraction. It seems that this length depends on the void and blockage fractions, and for blockage severity <40%, on the shape of the blockage.

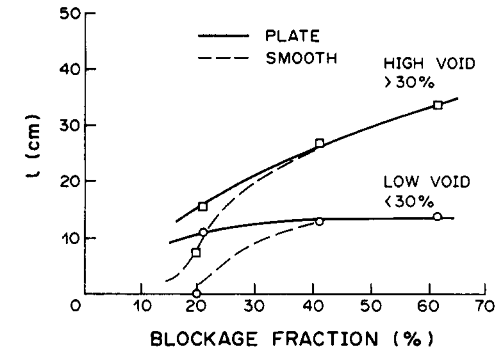

Figure 6. Variation of the high void region length with blockage severity.

5. CONTRACTION COEFFICIENT

In the derivation of irreversible pressure losses caused by inserts, [9] and [11], it was assumed that all pressure losses take place during the expansion from the vena contracta to the flow section of the tube. Consequently, the aforementioned equations contain, among other parameters, the contraction coefficient (C) and the void fraction at the vena contracta and far downstream of the blockage. Teyssedou (1987) measured the local void fraction profiles at different locations upstream and downstream of plate blockages of varying severities. He observed that the average void fraction in the contracted zone is quite close to the average void fraction in the channel. Therefore, in the determination of the contraction coefficient using data on the irreversible form pressure losses, it is assumed that the void fraction at the vena contracta is equal to the arithmetic average of the void fraction far upstream and downstream of the blockage.

Figure 7 gives the contraction coefficients calculated using the Janssen–Kervinen [10], and momentum–energy, [11], models. The contraction coefficients calculated with the two models agree well up to about 30% void fraction, after which increasing differences have been observed with

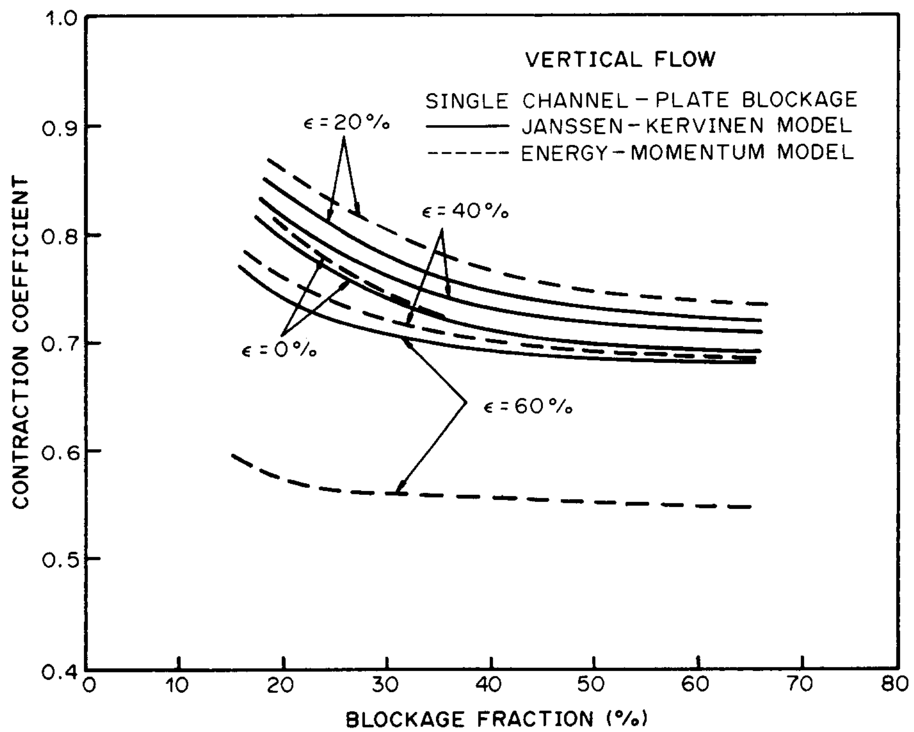

Figure 7. Contraction coefficients obtained with different two-phase flow models for plate blockages.

Table 2. Vena contracta coefficients and the location of the flow separation for smooth blockages

Blockage (%)	Average void ϵ_3	ϵ_4	Mass flux (kg/m^2 s)	Janssen–Kervinen model C	Z (mm)	Energy–momentum model C	Z (mm)
20.1	0.0	0.0	2078.2	1.100	14.91	1.100	14.91
20.1	0.21	0.21	2078.5	1.027	7.39	1.046	9.82
20.1	0.46	0.46	2079.1	0.910	0.0	0.767	0.0
20.1	0.60	0.60	2074.6	0.838	0.0	0.538	0.0
41.4	0.0	0.0	2073.0	1.283	15.02	1.283	15.02
41.4	0.21	0.21	2081.1	1.130	9.92	1.145	10.53
41.4	0.46	0.46	2078.1	0.946	0.0	0.827	0.0
41.4	0.60	0.60	2070.7	0.811	0.0	0.578	0.0
59.5	0.0	0.0	2068.4	1.375	11.78	1.375	11.78
59.5	0.0	0.0	3089.4	1.391	12.03	1.391	12.03
59.5	0.21	0.21	2072.6	1.118	6.74	1.134	7.14
59.5	0.40	0.40	2072.7	0.950	0.0	0.934	0.0
59.5	0.61	0.61	2065.0	0.829	0.0	0.638	0.0
59.5	0.46	0.46	2069.1	0.924	0.0	0.831	0.0

increasing void fractions. At this stage, it is rather difficult to decide which contraction coefficient is more realistic without carrying out further experiments aimed at determining the extent of the vena contracta. Therefore, the best approach is to use the contraction coefficient from figure 7 corresponding to the model chosen. It is also observed that the C-coefficients obtained under two-phase flow conditions differ somewhat from those obtained under single-phase flow conditions. In both cases, this coefficient shows a clear tendency towards unity as the blockage fraction goes to zero. For blockage fractions >40%, the decrease in the contraction coefficient with increasing blockage fraction is quite slow.

Equations [10] and [12] have also been employed to determine the C-coefficients for smooth blockages. This coefficient is defined as the ratio of the flow area in the vena contracta to that in the mid-plane of the blockage [figure 4(b)] and by definition should have values <1. The resulting C-coefficients are shown in table 2 and in half of the runs they are >1. The values >1 are interpreted as indicating that there is no formation of vena contracta. However, the flow may separate from the blockage surface in the downstream region of the mid-plane [plane 3 in figure 4(a)]. It can be assumed that all the irreversible form pressure loss takes place during the expansion from the flow section corresponding to the separation point, A_3, to the flow section of the channel, A_4 [see figure 4(a)]. The value of the flow section A_3, i.e. the point where the flow separates from the surface of the blockage, has been estimated by setting $C = 1$ in the theoretical model, [10]. The distance of the separation point (Z) to the mid-plane of the blockage is also given in table 2. Values of $C < 1$ may be interpreted as indicating the existence of a vena contracta. As illustrated in figure 8, the C-coefficients calculated with the momentum–energy model differ appreciably from those of the Janssen–Kervinen model.

6. IRREVERSIBLE PRESSURE DROP COEFFICIENT

The irreversible pressure drop caused by inserts can be written as

$$\Delta p_{\mathrm{form,\,TP}} = -K_{\mathrm{TP}}\frac{G^2}{2\rho'} \qquad [14]$$

and by comparing [14] with [10], the relationship between K_{TP} and the contraction coefficient is easily obtained:

$$K_{\mathrm{TP}} = \left(\frac{1}{\sigma C} - 1\right)^2. \qquad [15]$$

Using the form pressure loss and void fraction data given by Tapucu *et al.* (1988), the irreversible pressure loss coefficient (K_{TP}) appearing in [14] has been calculated for plate and smooth blockages. The variations of this coefficient for both blockages as a function of the void fraction for a given

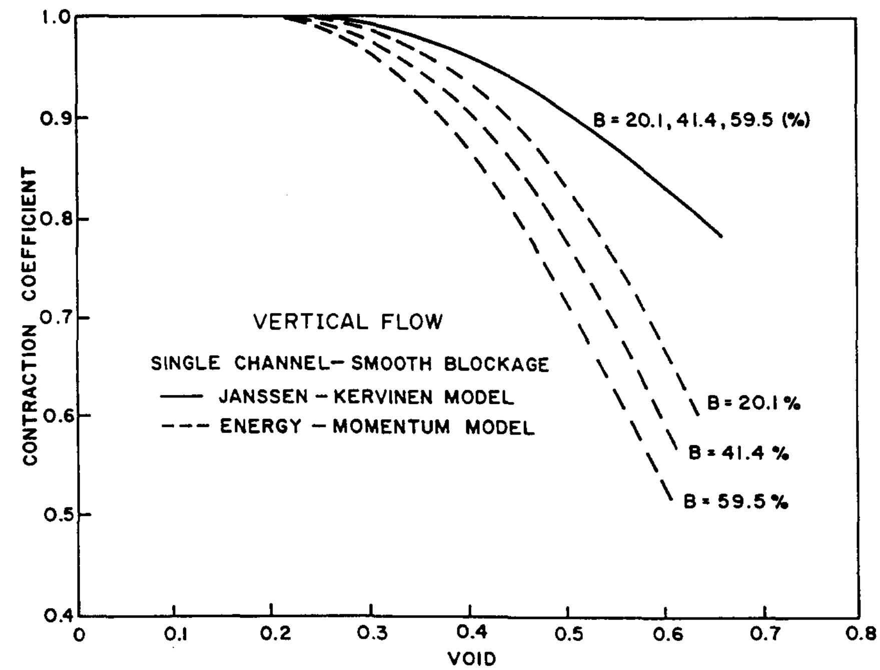

Figure 8. Contraction coefficients obtained with different two-phase flow models for smooth blockages.

blockage fraction and as a function of the blockage fraction for a given void fraction are shown in figures 9–11.

For plate blockages, at a given blockage fraction, the irreversible pressure loss coefficient first decreases with increasing void fraction and then increases (figure 9). However, the overall changes, within the range of void fractions studied (0–60%), were rather small. Therefore, the dependency of this coefficient on void fraction can be considered as weak. On the other hand, as illustrated in figure 11, the K_{TP}-coefficient increases rapidly with increasing blockage fraction.

For smooth blockages, the irreversible pressure loss coefficient increases with increasing void and blockage fractions (figures 10 and 11). Figure 11 also compares the K_{TP}-coefficient obtained for

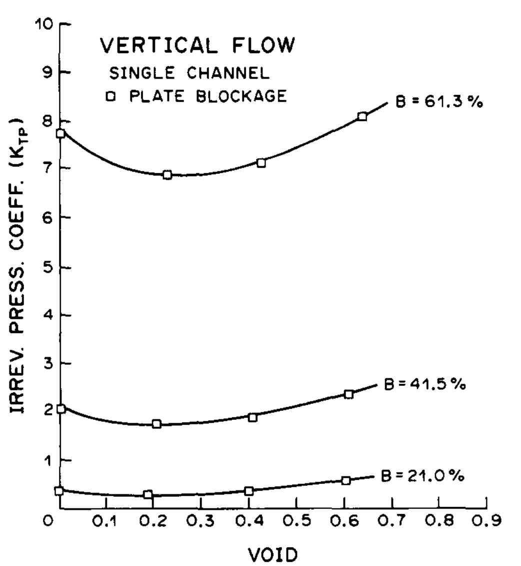

Figure 9. Irreversible pressure loss coefficient for plate blockages.

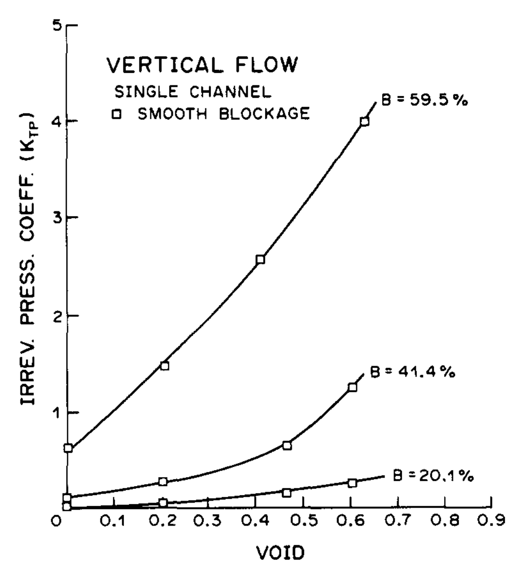

Figure 10. Irreversible pressure loss coefficient for smooth blockages.

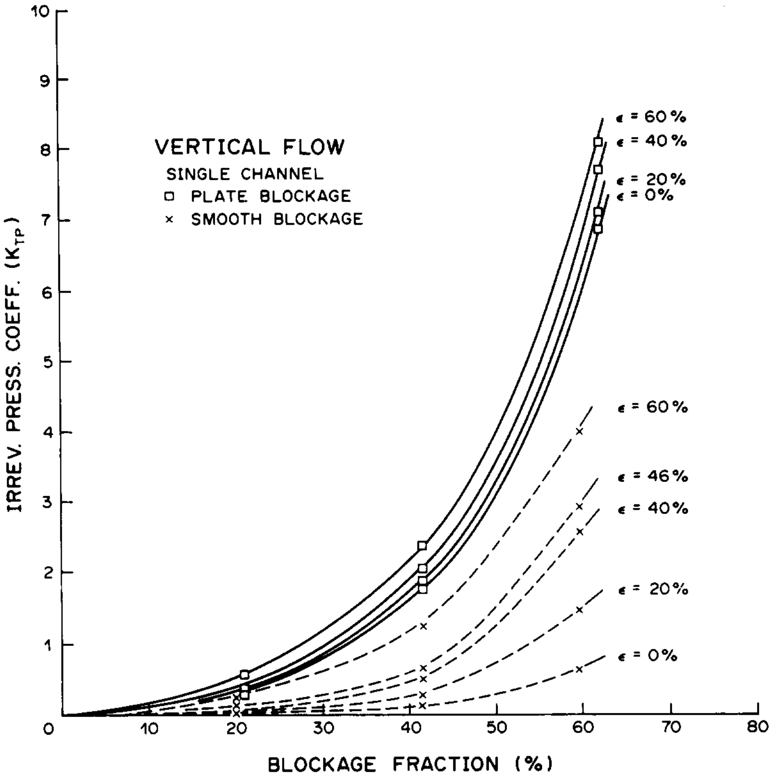

Figure 11. Irreversible pressure loss coefficients for plate and smooth blockages.

plate and smooth blockages. It is observed that smooth blockages yield substantially lower K_{TP}-coefficients than plate blockages.

Defining the form two-phase multiplier as

$$\phi^2_{\text{form}} = \frac{\Delta p_{\text{form, TP}}}{\Delta p_{\text{form, SP}}} \qquad [16]$$

and using [14] for single- and two-phase flows, the above equation can be written as

$$\Phi^2_{\text{form}} = \frac{K_{TP}}{K_{SP}}\frac{\rho_L}{\rho'}. \qquad [17]$$

The variation of ϕ^2_{form} with blockage fraction is shown in figures 12 and 13 for plate and smooth blockages, respectively. No data have been collected for blockage fractions <20%. However, since the contraction coefficients for single- and two-phase flows seem to tend toward unity simultaneously when the blockage approaches zero (figure 7), by using [15] it can be seen that K_{TP}/K_{SP} would tend toward unity and Φ^2_{form} toward ρ_L/ρ'. The variation of this multiplier with the flow dryness fraction for sharp and smooth blockages is given in figure 14. The higher values of Φ^2_{form} observed for smooth blockages are simply the consequence of the small pressure losses caused by smooth blockages under single-phase flow conditions. Figure 14 also compares the two-phase multipliers obtained for plate blockages with those for orifices used by Simpson *et al.* (1979). The plate blockages seem to yield somewhat higher values than the orifices.

7. CONCLUSIONS

In this paper the irreversible form pressure losses caused by plate and smooth blockages for air–water flows close to atmospheric pressure conditions have been investigated. Visual observation of the blocked region showed that a recirculation zone forms on both sides of the blockage. The upstream recirculation zone is small and rich in liquid, whereas the downstream recirculation zone is large and has a high void content.

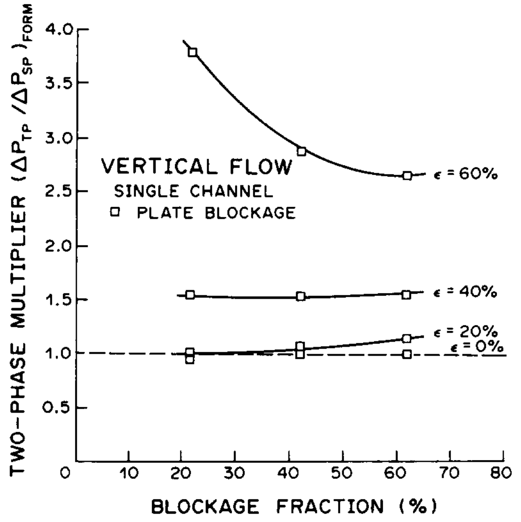

Figure 12. Form two-phase multiplier for plate blockages.

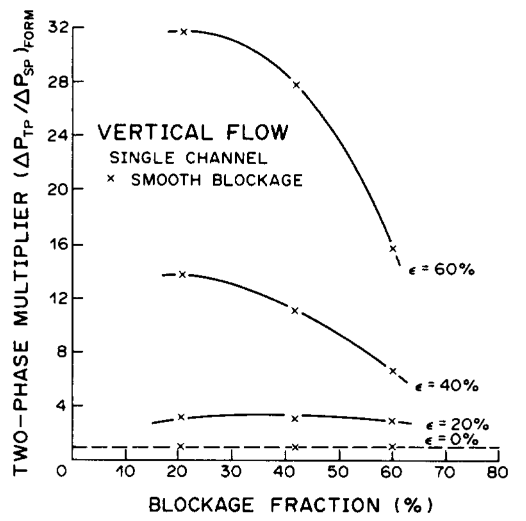

Figure 13. Form two-phase multiplier for smooth blockages.

The Janssen–Kervinen and the momentum–energy models were used to calculate the vena contracta coefficients for plate and smooth blockages. Since for the present experimental conditions the compressibility effects of the gas were negligible, the above models were used with the assumption that the flow was incompressible. No attempt was made to take into account the liquid entrained by the gas (Morris 1984), since such an approach requires an additional parameter—the entrainment coefficient.

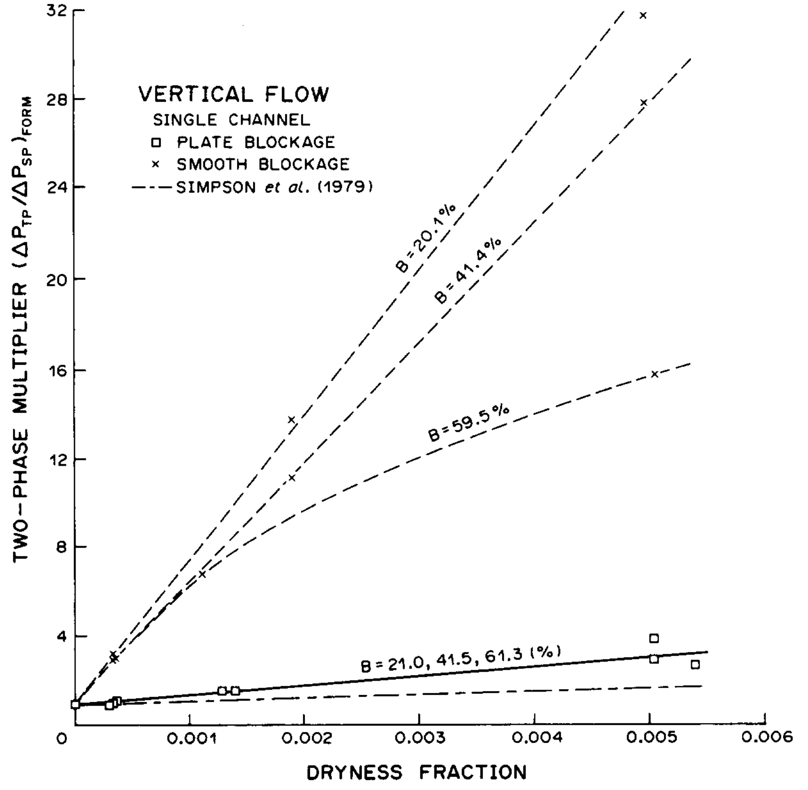

Figure 14. Form two-phase multipliers for plate and smooth blockages and comparison with orifice restrictions (Simpson *et al.* 1979).

The vena contracta coefficients for plate blockages determined using the Janssen–Kervinen and momentum–energy models agree well up to about 30% void fraction. It is observed that the contraction coefficients obtained under two-phase flow conditions differ somewhat from those obtained under single-phase flow conditions.

The irreversible form pressure loss coefficients determined for plate and smooth blockages depend on blockage severity and void fraction. However, for plate blockages the dependence of this coefficient on void fraction is rather weak.

NOMENCLATURE

A = Flow area (m^2)
C = Vena contracta coefficient
G = Mass flux ($kg/m^2\,s$)
K = Irreversible pressure loss coefficient
g = Acceleration of gravity (m/s^2)
p = Pressure (Pa)
v' = Momentum specific volume (m^3/kg)
v_e = Effective specific volume (m^3/kg)
x = Dryness fraction
z = Axial distance (m)
ϵ = Void fraction
P_w = Perimeter (m)
Δp = Pressure drop (Pa)
Δp_{accel} = Acceleration pressure drop (Pa)
Δp_b = Total pressure drop caused by the blockage (Pa)
Δp_{form} = Form pressure loss (Pa)
$\Delta p_{friction}$ = Friction pressure loss (Pa)
$\Delta p_{gravity}$ = Gravity pressure loss (Pa)
ρ = Density (kg/m^3)
$\bar{\rho}$ = Two-phase mixture density, $\epsilon\rho_G + (1-\epsilon)\rho_L$ (kg/m^3)
ρ_H = Homogeneous two-phase specific density (kg/m^3)
σ = Area ratio (A_1/A_2)
τ_W = Wall shear stress (N/m^2)
ϕ' = Viscous dissipation ($J/m^2\,s$)
Φ^2_{form} = Two-phase form multiplier
Φ^2_L = Two-phase multiplier

Subscripts

G = Gas
L = Liquid
TP = Two-phase
SP = Single phase

Acknowledgements—We are grateful to Mssrs P. Champagne and R. Desjardins for their technical contributions. This work was funded by the Electric Power Research Institute, Calif., U.S.A.

REFERENCES

BIZON, E. 1965 Two-phase flow measurement with sharp-edged orifices and venturis. Report AECL-2273.

CHEN, D. K., CHEN, Z. H., ZHAQ, Z. S. & ZHUO, N. 1986 The local resistance of gas–liquid two-phase flow through an orifice. *Int. J. Heat Fluid Flow* **7**, 231–238.

CHISHOLM, D. 1967a Flow of incompressible two-phase mixtures through sharp-edged orifices. *J. mech. Engng Sci.* **9**, 72–78.

CHISHOLM, D. 1967b Flow of incompressible two-phase mixtures through throttling devices. *Chem. Process Engng* **48,** 73–78.

CHISHOLM, D. 1983 *Two-phase Flow in Pipelines and Heat Exchangers* (Edited by GOODWIN, G.). Institution of Chemical Engineers, London.

CHISHOLM, D. & WATSON, G. G. 1965 The flow of steam–water mixtures through sharp-edge orifices. Presented at *Symp. Two-phase Flow*, Univ. of Exeter, Devon.

COLLIER, J. G. 1972 *Convective Boiling and Condensation.* McGraw-Hill, New York.

DELHAYE, J. M. 1981 *Two-phase Flow and Heat Transfer in the Power and Process Industries.* Hemisphere, Washington, D.C.

FAIRHURST, C. P. 1983 Component pressure loss during two-phase flow. In *Proc. Int. Conf. Physical Modelling of Multi-phase Flow*, Coventry, W. Midlands, pp. 1–24.

HEWITT, G. F. & HALL TAYLOR, N. S. 1970 *Annular Two-phase Flow.* Pergamon Press, Oxford.

Hoopes, J. W. 1957 Flow of steam–water mixtures in a heated annulus and through orifices. *A.I.Ch.E. Jl* **3,** 268–275.

JANSSEN, E. & KERVINEN, J. A. 1964 Two-phase pressure drop across contractions and expansions, water–steam mixtures at 600–1400 psia. Report GEAP-4622.

KAYS, W. M. 1950 Loss coefficient for abrupt changes in flow cross section with low Reynolds number flow in single and multiple-tube systems. *Trans. ASME* **72,** 1067–1074.

MONROE, E. S. 1958 Flow of saturated boiler water through knife-edge orifices in series. *Trans. ASME* **78,** 373–377.

MORRIS, D. S. 1984 A simple model for estimating two-phase momentum flux. Presented at the *1st U.K. Natn. Conf. Heat Transfer*, Univ. of Leeds (Edited by the INSTITUTION OF CHEMICAL ENGINEERS), pp. 773–784. Pergamon Press, New York.

SALCUDEAN, M., GROENEVELD, D. C. & LEUNG, L. 1983a Effect of flow obstruction geometry on pressure drops in horizontal air–water flow. *Int. J. Multiphase Flow* **9,** 73–85.

SALCUDEAN, M., CHUN, J. H. & GROENVELD, D. C. 1983b Effect of flow-obstruction on the flow pattern transitions in horizontal two-phase flow. *Int. J. Multiphase Flow* **9,** 91–96.

SALCUDEAN, M., CHUN, J. H. & GROENEVELD, D. C. 1983c Effect of flow obstruction on void distribution in horizontal air–water flow. *Int. J. Multiphase Flow* **9,** 87–90.

SIMPSON, H. C., ROONEY, D. H. & GRATTAN, E. 1979 Two-phase pressure drop in valve and orifice restrictions. Presented at the *European Two-phase Flow Gp Mtg*, Ispra, Italy.

SIMPSON, H. C., ROONEY, D. H. & GRATTAN, E. 1983 Two-phase flow through gate valves and orifice plates. In *Proc. Int. Conf. Physical Modelling of Multi-phase Flow*, Coventry, W. Midlands, pp. 25–40.

TAPUCU, A., TEYSSEDOU, A., GECKINLI, M. & TROUCHE, N. 1988 Experimental study of the diversion cross-flow caused by subchannel blockages. Part II: two phase flow. Report EPRI NP-3459, Vol. 2.

TEYSSEDOU, A. 1987 Thermo-hydraulic behavior of interconnected subchannels with blockages. Ph.D. Thesis, Ecole Polytechnique de Montréal, Québec.

THOM, J. R. S. 1963 The flow of a steam–water mixture through sharp-edged orifices. Babcock & Wilcox Report No 1/62/65.

WEISMAN, J., HUSAIN, A. & HARSHE, B. 1978 Two-phase pressure drop across abrupt area changes and restrictions. In *Proceedings of the Two-phase and Heat Transfer Symposium* (Edited by VEZIROGLU, T. N. & KAKAÇ, S.), pp. 1281–1316. Hemisphere, Washington, D.C.